Description of the isotope chain $^{180-196}$Pt within some solvable approaches

A. A. Raduta[a,b] and P. Buganu[a]

[a)] *Department of Theoretical Physics,*

Institute of Physics and Nuclear Engineering,

POBox MG6, Bucharest 077125, Romania and

[b)] *Academy of Romanian Scientists, 54 Splaiul Independentei, Bucharest 050094, Romania*

Abstract

Energies of the ground, β and γ bands as well as the associated B(E2) values are determined for each even-even isotope of the $^{180-196}$Pt chain by the exact solutions of some differential equations which approximate the generalized Bohr-Mottelson Hamiltonian. The emerging approaches are called the Sextic and Spheroidal Approach (SSA), the Sextic and Mathieu Approach (SMA), the Infinite Square Well and Spheroidal Approach (ISWSA) and the Infinite Square Well and Mathieu Approach (ISWMA), respectively. While the first three methods were formulated in some earlier papers of the present authors, ISWMA is an inedit approach of this work. Numerical results are compared with those obtained with the so called X(5) and Z(5) models. A contour plot for the probability density as function of the intrinsic dynamic deformations is given for a few states of the three considered bands with the aim of evidencing the shape evolution along the isotope chain and pointing out possible shape coexistence.

PACS numbers: 21.10.Re, 21.60.Ev, 27.70.+q

I. INTRODUCTION

Since the critical point symmetries [2–5] of the nuclear shape phase transitions were proposed, many experimental and theoretical efforts were made to find the nuclei described by the new symmetries. While at the beginning the X(5) [3] candidates were found in the mass region of $A \approx 150$ [6–8], recently a new region has been suggested for Os and Pt isotopes with $A \approx 180$ [9, 10]. In Refs. [11, 12] data for the isotopes ^{176,178,180,188,190,192}Os were analyzed with the Sextic and Spheroidal Approach (SSA) [11], the Davidson and Spheroidal Approach (DSA) [12], the Infinite Square Well and Spheroidal Approach (ISWSA) [13] and the results were compared with those of the Coherent State Model (CSM) [14] and X(5). According to our analysis these isotopes present features for the $U(5) \rightarrow SU(3)$ shape phase transition with the critical point reached for ^{176}Os and ^{188}Os. On the other hand, applying the Sextic and Mathieu Approach (SMA) [15] to ^{188,190,192}Os, one points out that the isotope ^{192}Os is a good candidate for the critical point of the phase transition between the prolate and the oblate shapes through the triaxial shape corresponding to $\gamma_0 = 30^0$.

Encouraged by the results for the Os isotopes, we consider the above mentioned models also for the even-even $^{180-196}$Pt isotopes. We aim not only at determining the energy spectra and the electric transition probabilities but also at showing the static deformation of each isotope in both the ground and excited states. New features like the shape coexistence or a transition from the prolate to oblate shapes through a triaxial deformation are expected to show up. Keeping in mind that the SMA, the ISWMA and the Z(5) [5] are suitable for the description of the triaxial nuclei lying close to $\gamma_0 = 30^0$, a comparison of their predictions represent a challenging task. ISWMA is the inedit model proposed in this paper.

Recently, in Ref. [10] it was shown that the isotope ^{182}Pt has some of the X(5) features. According to the Interacting Boson Model-1 (IBM-1) [16] and the General Collective Model [17] this isotope manifests shape coexistence and it is close to the critical point of the $U(5) \rightarrow SU(3)$ shape phase transition. Evidences for shape coexistence were also presented for ^{176,178}Pt [18, 19], ^{184}Pt [20], ^{186}Pt [21] and ^{188}Pt [22], which suggests that this behavior is a specific feature for Pt isotopes. Some investigations where the ground state shape evolution in Pt isotope chain from the prolate towards the oblate shapes were performed in Refs. [23, 24].

The objectives formulated above are achieved according to the following plan. In Section

II, a short presentation of the formalisms used for the description of the Pt even-even isotopes is given. Numerical results and their comparison with the corresponding experimental data are discussed in Section III. The final conclusions are drawn in Section IV.

II. SHORT PRESENTATION OF THE MODELS

The formalisms X(5), Z(5), ISWSA, ISWMA, SSA and SMA are derived by a set of approximations applied to the Bohr-Mottelson Hamiltonian [1],

$$H = -\frac{\hbar^2}{2B}\left[\frac{1}{\beta^4}\frac{\partial}{\partial\beta}\beta^4\frac{\partial}{\partial\beta} + \frac{1}{\beta^2\sin 3\gamma}\frac{\partial}{\partial\gamma}\sin 3\gamma\frac{\partial}{\partial\gamma} - \frac{1}{4\beta^2}\sum_{k=1}^{3}\frac{\hat{Q}_k^2}{\sin^2(\gamma-\frac{2\pi}{3}k)}\right] + C\frac{\beta^2}{2}, \quad (2.1)$$

amended with a potential [25, 26]

$$V(\beta,\gamma) = V_1(\beta) + \frac{V_2(\gamma)}{\beta^2}. \quad (2.2)$$

The form of the β and γ potential allows to separate the β variable from the γ and the three Euler angles θ_1, θ_2 and θ_3. Here, $\hat{Q}_k$'s denote the angular momentum components in the intrinsic reference frame. A full separation may be however achieved by expanding the rotor term in power series of γ around either of $\gamma_0 = 0$ or of $\gamma_0 = \pi/6$ and moreover by replacing the factor β^2 multiplying the γ-dependent term with its average value denoted hereafter by $\langle\beta^2\rangle$. The resulting equations are:

$$\left[-\frac{1}{\beta^4}\frac{d}{d\beta}\beta^4\frac{d}{d\beta} + \frac{\Lambda}{\beta^2} + v_1(\beta)\right] f(\beta) = \varepsilon_\beta f(\beta), \quad (2.3)$$

$$\left[-\frac{1}{\sin 3\gamma}\frac{d}{d\gamma}\sin 3\gamma\frac{d}{d\gamma} - W + v_2(\gamma)\right]\phi(\gamma) = \tilde{\varepsilon}_\gamma\phi(\gamma), \quad (2.4)$$

where the following notations are used:

$$v_1(\beta) = \frac{2B}{\hbar^2}V_1(\beta), \quad v_2(\gamma) = \frac{2B}{\hbar^2}V_2(\gamma), \quad \varepsilon_\beta = \frac{2B}{\hbar^2}E_\beta, \quad \tilde{\varepsilon}_\gamma = \langle\beta^2\rangle\frac{2B}{\hbar^2}E_\gamma. \quad (2.5)$$

Λ and W are the contributions coming from the rotor term and their expressions depend on the order of the γ series truncation.

For the sake of fixing the notations and defining the main ingredients, in what follows the above mentioned approaches will be briefly described. For details we advise the reader to consult Refs. [3, 5, 11–13, 15, 25, 26]. In Eq. (2.3), the X(5), Z(5), ISWSA and ISWMA models use a common potential in β, namely an infinite square well

$$v_1(\beta) = \begin{cases} 0, & \beta \le \beta_\omega \\ \infty, & \beta > \beta_\omega \end{cases}. \quad (2.6)$$

With such a choice Eq. (2.3) admits the Bessel functions of irrational order ν, as solutions:

$$f_{s,L}(\beta) = C_{s,L}\beta^{-\frac{3}{2}}J_{\nu}\left(\frac{x_{s,L}}{\beta_{\omega}}\beta\right), \quad s = 1, 2, 3, ... \tag{2.7}$$

$C_{s,L}$ denotes the normalization factor, $x_{s,L}$ the Bessel function zeros, while L is the total intrinsic angular momentum.

By contrast the SSA and SMA, use in Eq. (2.3) a sextic oscillator plus a centrifugal barrier potential [27],

$$v_1^{\pm}(\beta) = (b^2 - 4ac^{\pm})\beta^2 + 2ab\beta^4 + a^2\beta^6 + u_0^{\pm}, \;\; c^{\pm} = \frac{L}{2} + \frac{5}{4} + M, \; M = 0, 1, 2, ... \tag{2.8}$$

Here, $c^{\pm}$ has two different values, one for L even and other for L odd, while $u_0^{\pm}$ are constants which are fixed such that the two potentials v_1^{+} and v_1^{-} have the same minimum energy. Eq. (2.3), with $\Lambda = L(L+1) - 2$ and the potential given by Eq. (2.8), is quasi-exactly solved, the solutions being of the form:

$$\varphi_{n_\beta,L}^{(M)}(\beta) = N_{n_\beta,L}P_{n_\beta,L}^{(M)}(\beta^2)\beta^{L+1}e^{-\frac{a}{4}\beta^4 - \frac{b}{2}\beta^2}, \;\; n_\beta = 0, 1, 2, ...M, \tag{2.9}$$

where $N_{n_\beta,L}$ is the normalization factor, while $P_{n_\beta,L}^{(M)}(\beta^2)$ are polynomials of order n_β in β^2.

Concerning the Eq. (2.4), the X(5) and Z(5) chose an oscillator and a shifted oscillator potential, respectively:

$$v_2(\gamma) = c\frac{1}{2}(\gamma - \gamma_0)^2. \tag{2.10}$$

Indeed $\gamma_0 = 0$, for X(5), and $\gamma_0 = \pi/6$ for Z(5). The solutions of Eq. (2.4) are the generalized Laguerre polynomials, L_n^m , if $\gamma_0 = 0$

$$\eta_{n_\gamma,K}(\gamma) = C_{n,K}\gamma^{|K/2|}e^{-(3a)\gamma^2/2}L_n^{|K|}(3a\gamma^2), n = \left(\frac{n_\gamma - |K|}{2}\right), \; a = \frac{\sqrt{c}}{3}, \;\; n_\gamma = 0, 1, 2, ... \tag{2.11}$$

The quantum number K corresponds to the angular momentum projection on the intrinsic z-axis. and the Hermite polynomials H_n, for $\gamma_0 = \pi/6$

$$\eta_{\bar{n}_\gamma} = N_{\bar{n}_\gamma}H_{\bar{n}_\gamma}(b(\gamma - \pi/6))e^{-b^2(\gamma-\pi/6)/2}, \; b = \left(\frac{c\langle\beta^2\rangle}{2}\right)^{1/4}, \; \bar{n}_\gamma = 0, 1, 2, ..., \tag{2.12}$$

Both models, the X(5) and the Z(5), consider in Eq. (2.4) a zeroth order of approximation for the rotor term.

This is not the case for the ISWSA, ISWMA, SSA and SMA models, where a second order power expansion of both the the rotor term and the periodic potential

$$v_2(\gamma) = u_1\cos 3\gamma + u_2\cos^2 3\gamma, \tag{2.13}$$

is used, which results of having the spheroidal ($S_{m,n}$) and Mathieu ($\mathcal{M}_n$) functions as solutions of the resulting differential equations, respectively:

$$\eta(\gamma) = S_{m,n}(\cos 3\gamma; c),\ \eta(\gamma) = \frac{\mathcal{M}_n(3\gamma; q)}{\sqrt{|\sin 3\gamma|}}. \tag{2.14}$$

The expressions of c and q will be specified below.

The advantages of the Mathieu and spheroidal functions consist of that they are periodic, defined on a bound interval and normalized to unity with the integration measure of $|\sin 3\gamma| d\gamma$, preserving in this way the hermiticity of the initial Hamiltonian. Note that the other approaches do not satisfy these conditions.

The total energy of the system is obtained by summing the eigenvalues of the β and γ equations:

$$\varepsilon = \varepsilon_\beta + \tilde{\varepsilon}_\gamma. \tag{2.15}$$

The excitation energies yielded by the formalisms used in the present paper, are as follows:

$$\textbf{X(5):}\ E(s, L, n_\gamma, K) - E(1,0,0,0) = B_1(x^2_{s,L} - x^2_{1,0}) + \delta_{K,2}X,\ X = A_1 + 4C_1, \tag{2.16}$$

with A_1, B_1 and C_1 arbitrary parameters. In our calcultions the parameter X is fitted.

$$\textbf{Z(5):}\ E(s, L, n_\gamma = 0, R) - E(1,0,0,0) = B_1(x^2_{s,L,R} - x^2_{1,0,0}),\ B_1 = \frac{1}{\beta^2_\omega}\frac{\hbar^2}{2B}, \tag{2.17}$$

$$\begin{aligned}
\textbf{ISWSA:}\quad & E(s, n_\gamma, m_\gamma, L, K) = B_1 x^2_{s,L} + F\left[9\lambda_{m_\gamma,n_\gamma}(c) + \frac{u_1}{2} + \frac{11}{27}D - \frac{L(L+1)}{3}\right], \\
& \lambda_{m_\gamma,n_\gamma} = \frac{1}{9}\left[\tilde{\varepsilon}_\gamma - \frac{u_1}{2} - \frac{11}{27}D + \frac{1}{3}L(L+1)\right],\ c^2 = \frac{1}{9}\left(\frac{u_1}{2} + u_2 - \frac{2}{27}D\right), \\
& m_\gamma = \frac{K}{2},\ \ D = L(L+1) - K^2 - 2,\ F = \frac{1}{\langle\beta^2\rangle}\frac{\hbar^2}{2B},
\end{aligned} \tag{2.18}$$

$$\begin{aligned}
\textbf{ISWMA:}\quad & E(s, n_\gamma, L, R) = B_1 x^2_{s,L} + F\left[9a_{n_\gamma}(L,R) + 18q(L,R) - \frac{3}{4}R^2 - \frac{5}{2}\right], \\
& q = \frac{1}{36}\left(\frac{10}{9}L(L+1) - \frac{13}{12}R^2 + u_1 - \frac{9}{4}\right),\ a_{n_\gamma} = \frac{1}{9}\left(\tilde{\varepsilon}_\gamma + \frac{3}{4}R^2 + \frac{5}{2}\right) - 2q,
\end{aligned} \tag{2.19}$$

SSA:

$$\begin{aligned}
& E(n_\beta, n_\gamma, m_\gamma, L, K) = E\left[b(2L+3) + \lambda^{(M)}_{n_\beta} + u^{\pm}_0\right] + F\left[9\lambda_{m_\beta,n_\gamma}(c) + \frac{u_1}{2} + \frac{11}{27}D - L(L+1)\right], \\
& \lambda_{m_\gamma,n_\gamma} = \frac{1}{9}\left[\tilde{\varepsilon}_\gamma - \frac{u_1}{2} - \frac{11}{27}D + \frac{1}{3}L(L+1)\right] + \frac{2L(L+1)}{27},\ E = \frac{\hbar^2}{2B},
\end{aligned} \tag{2.20}$$

SMA: (2.21)

$$E(n_\beta, n_\gamma, L, R) = E\left[4bs(L) + \lambda^{(M)}_{n_\beta}(L) + u^\pi_0\right] + F\left[9a_{n_\gamma}(L,R) + 18q(L,R) - \frac{3}{4}R^2 - \frac{5}{2}\right],$$

where $\lambda^{(M)}_{n_\beta}(L)$ satisfy the equation:

$$\left[-\left(\frac{d^2}{d\beta^2} + \frac{4s-1}{\beta}\frac{d}{d\beta}\right) + 2b\beta\frac{d}{d\beta} + 2a\beta^2\left(\beta\frac{d}{d\beta} - 2M\right)\right] P^{(M)}_{n_\beta,L}(\beta^2) = \lambda^{(M)}_{n_\beta} P^{(M)}_{n_\beta,L}(\beta^2). \quad (2.22)$$

The reduced E2 transition probabilities for ISWSA and SSA are determined with the reduced matrix element of the transition operator:

$$T^{(E2)}_{2\mu} = t_1\beta\left[\cos\gamma D^2_{\mu 0} + \frac{\sin\gamma}{\sqrt{2}}(D^2_{\mu 2} + D^2_{\mu,-2})\right] + t_2\sqrt{\frac{2}{7}}\beta^2\left[-\cos 2\gamma D^2_{\mu 0} + \frac{\sin 2\gamma}{\sqrt{2}}(D^2_{\mu 2} + D^2_{\mu,-2})\right], \quad (2.23)$$

between the corresponding initial $|L_i M_i\rangle$ and final $|L_f M_f\rangle$ states, as described above:

$$B(E2; L_i \to L_f) = |\langle L_i||T^{(E2)}_2||L_f\rangle|^2. \quad (2.24)$$

Here the Rose's convention [28] was used for the reduced matrix elements. For SMA, ISWMA and Z(5), in the expression of the transition operator (2.23) γ is substituted with $\gamma - 2\pi/3$. The argument is justified by the fact that $\gamma - 2\pi/3$ defines the axis 1 of the principal inertial ellipsoid. Indeed, the transformation from the laboratory to the intrinsic frame is a rotation defined by the matrix D^L_{MR}, where M and R are eigenvalues of the operator $\hat{Q}_1$. The X(5) and Z(5) models keep only the zero order approximation of the first γ-term in the transition operator (2.23).

III. NUMERICAL RESULTS

The formalisms presented in Section II were applied to some even-even isotopes of Pt: $^{180-196}$Pt. It is commonly accepted that nuclear spectra can be classified by the values of the energy ratios:

$$\begin{aligned} R_{4^+_g/2^+_g} &= \frac{E_{4^+_g} - E_{0^+_g}}{E_{2^+_g} - E_{0^+_g}}, \\ R_{0^+_\beta/2^+_g} &= \frac{E_{0^+_\beta} - E_{0^+_g}}{E_{2^+_g} - E_{0^+_g}}. \end{aligned} \quad (3.1)$$

Moreover, it seems that nuclei satisfying a certain symmetry are characterized by almost constant ratios. The values of these ratios associated to the isotopes considered here are

collected in Table I. As seen from there, the ratios $R_{4_g^+/2_g^+}$ for ^{180,182,184}Pt are close to that predicted by the $X(5)$ approach. By contrast the other ratio $R_{0_\beta^+/2_g^+}$ indicates that these isotopes are far from the ideal picture of $X(5)$. As a matter of fact this feature is consistent with the results of Ref.[29] saying that not all nuclear properties reach the critical point in a phase transition in the same isotope. We apply the approaches ISWSA and SSA to the mentioned isotopes in order to test their ability to account for these complementary features.

Concerning the description called $Z(5)$ this is appropriate for ^{190,192,194,196}Pt, the statement being supported by the values of both ratios. Indeed, the detailed numerical analysis of Ref.[5] shows a good agreement between calculations and experimental data. In this context the application of the ISWMA and SMA to these isotopes will provide a sensible comparison of the formalisms on one hand and the $Z(5)$ on the other hand.

It is well known that the triaxial rigid rotor (TRR) predicts [30] a relation between the first three excited state energies:

$$\triangle E \equiv E_{3_\gamma^+} - E_{2_\gamma^+} - E_{2_g^+} = 0. \tag{3.2}$$

Due to this fact the above equation is considered to be a signature for a triaxial deformation of $\gamma_0 = 30^0$. For the isotope ^{192}Pt the above equation reads: $|\Delta E| = 8$ keV, which means that the mentioned isotope is close to the ideal triaxial rigid rotor. Considering this isotope among the treated isotopes allows us to answer the question whether these approaches are suitable for the description of the triaxial nuclei. The isotopes ^{186,188,190,192,194,196}Pt may be considered to be $\gamma-$unstable nuclei, having the ratio $R_{4_g^+/2_g^+}$ close to 2.5. A special case is that of ^{186}Pt which has the had state of gamma band higher in energy than the first beta state which result in claiming a gamma stable picture. Most likely this nucleus exhibits the main features for the critical point of the phase transition from prolate to oblate shapes. Due to the specific structure of their potentials in the γ variable, the ISWSA and SSA seem to be suitable to describe both the $\gamma-$unstable and $\gamma-$stable deformed nuclei. Actually this argument justifies including ^{186}Pt and ^{188}Pt on the list of considered isotopes.

Each approach involves a number of free parameters for energies as well as for B(E2) values. These are fixed by fitting some particular experimental data concerning either the excitation energies or the reduced transition probabilities. The results of the fitting procedure adopted are listed in Tables II$-$VII.

Numerical results for the excitation energies of the ground, β and γ bands, as well as

TABLE I: Signatures of X(5), Z(5) and O(6) symmetries identified in the even-even isotopes $^{180-196}$Pt. The two ratios are defined by Eq.(3.1).

	^{180}Pt	^{182}Pt	^{184}Pt	^{186}Pt	^{188}Pt	^{190}Pt	^{192}Pt	^{194}Pt	^{196}Pt	X(5)	Z(5)	O(6)
$R_{4_g^+/2_g^+}$	2.69	2.71	2.67	2.55	2.52	2.49	2.48	2.47	2.46	2.90	2.35	2.50
$R_{0_\beta^+/2_g^+}$	3.12	3.23	3.02	2.46	3.00	3.11	3.78	3.86	3.19	5.65	3.91	-

TABLE II: The X(5) parameters for the $^{180-184}$Pt isotopes, obtained by a fitting procedure.

X(5)	^{180}Pt	^{182}Pt	^{184}Pt
B_1 [keV]	19.08	18.02	17.28
X [keV]	722.5	720.7	739.7
t_1 [W.u.]$^{1/2}$	500.2	451.2	419.6

TABLE III: The parameters of the ISWSA approach determined by a fitting procedure for $^{180-188}$Pt.

ISWSA	^{180}Pt	^{182}Pt	^{184}Pt	^{186}Pt	^{188}Pt
B_1 [keV]	16.38	16.39	16.83	16.25	21.5
F [keV]	17.32	11.33	3.35	16.82	41.99
u_1	-0.15	-31.56	-1000	-253.8	-97.45
u_2	-104.6	-163	-1000	6.75	81.07
t_1 [W.u.]$^{1/2}$	614.4	2200	2422	1728	517.4
t_2[W.u.]$^{1/2}$	0	9062	11331	5978	0

for the quadrupole electric transitions between states of these bands are compared with the corresponding experimental data in Tables VIII−X and XI−XIII, respectively. For each formalism the agreement between the calculation results and the corresponding experimental data is quantitatively appraised by the r.m.s values of the deviations.

From Table VIII, one can see that spectra of the isotopes ^{180}Pt, ^{182}Pt and ^{184}Pt are better described by SSA and ISWSA than by X(5). The best approach seems to be SSA. Moreover, the X(5) failure in explaining the data from the β band is removed by SSA, and that happens especially for ^{182}Pt. Concerning the γ band, all three formalisms, SSA, ISWSA

TABLE IV: The same as in Table III, but for the SSA model.

SSA	^{180}Pt	^{182}Pt	^{184}Pt	^{186}Pt	^{188}Pt
E [keV]	1.04	0.81	0.62	0.85	1.45
F [keV]	3.34	5.33	6.25	3.08	14.55
a	1059	1687	3030	1296	1449
b	135	186	256	170	95
u_1	-821.2	-1042	-302.6	1471	-466.2
u_2	-1000	-0.0007	-262	-2326	165.8
t_1 [W.u.]$^{1/2}$	1750	6561	7821	5061	1717
t_2 [W.u.]$^{1/2}$	0	89567	122065	58515	0

TABLE V: The parameters characterizing Z(5), for $^{190-196}$Pt.

Z(5)	^{190}Pt	^{192}Pt	^{194}Pt	^{196}Pt
B_1 [keV]	28.12	29.45	32.65	31.49
t_1 [W.u.]$^{1/2}$	27.49	23.94	18.76	20.77

TABLE VI: The same as in Table V, but for the ISWMA model.

ISWMA	^{190}Pt	^{192}Pt	^{194}Pt	^{196}Pt
B_1 [keV]	16.73	17.84	19.87	18.27
F [keV]	12.82	13.98	18.43	9.98
u_1	26.67	9.49	5	56.53
t_1 [W.u.]$^{1/2}$	28.14	24.51	16.94	19.79
t_2 [W.u.]$^{1/2}$	0	102.4	137.6	172.9

and X(5), encounter difficulties in explaining the band had energy. A possible explanation would be that the state 2^+_γ, does not actually belong to the γ band. A similar situation is met in ^{186}Pt. In ^{188}Pt, however, all three bands considered here are realistically described by SSA.

The comparison of the numerical results yielded by SMA, ISWMA and Z(5) with experimental data for the even-even isotopes $^{190-196}$Pt, is made in Tables IX and X, with the

TABLE VII: The same as in Table V, but for the SMA model.

SMA	^{190}Pt	^{192}Pt	^{194}Pt	^{196}Pt
E [keV]	1.11	2.95	2.96	0.41
F [keV]	8.14	7.87	14.68	6.46
a	3014.12	616.5	733	28322
b	84	22.98	33.05	250
u_1	104.6	121.8	32.74	177.1
t_1 [W.u.]$^{1/2}$	96.38	55.10	43.42	130.2
t_2 [W.u.]$^{1/2}$	0	1048	968.6	7708

result in favor of SMA and ISWMA.

The electromagnetic transition probabilities, calculated with Eq. (2.24), are included in Tables XI−XIII. Analyzing the r.m.s. values for each model, one may conclude that SSA and ISWSA describe the experimental data batter than X(5), while SMA and ISWMA better than Z(5). An explanation for this picture could be that X(5) and Z(5) use only the zero order approximation of the harmonic part of the transition operator (2.23). Indeed, as shown in Table XI, for ^{180}Pt the results obtained by SSA and ISWSA using only the harmonic transition operator are almost identical with those of X(5). By contrast for ^{182,184}Pt where the anharmonic contributions were included, the results of SSA and ISWSA are better than those of X(5). It is worth noticing that the r.m.s. associated to Z(5) for ^{192}Pt and ^{196}Pt are smaller than those provided by ISWMA. This situation might be caused by the fact the two approached considered for the γ band different descriptions. Indeed, in the framework of Z(5) the states of γ band are characterized by $n_\gamma = 0$ while the ISWMA γ states have $n_\gamma = 1$.

TABLE VIII: Excitation energies, given in units of keV, of the ground, β and γ bands states J_i^+ with $i = g, \beta, \gamma$, for ^{180,182,184}Pt yielded by the SSA, ISWSA and X(5) approaches, are compared with the corresponding experimental data taken from Refs. [31–33].

E [keV]	^{180}Pt				^{182}Pt				^{184}Pt			
J_i^+	Exp.	SSA	ISWSA	X(5)	Exp.	SSA	ISWSA	X(5)	Exp.	SSA	ISWSA	X(5)
2_g^+	153	126	125	133	155	139	121	126	163	131	119	121
4_g^+	411	386	366	387	420	412	353	366	436	393	347	351
6_g^+	757	749	693	724	775	778	666	684	798	749	650	656
8_g^+	1182	1194	1093	1131	1206	1216	1047	1069	1231	1176	1018	1025
10_g^+	1674	1705	1563	1604	1698	1710	1492	1515	1707	1658	1445	1453
12_g^+	2229	2273	2100	2139	2242	2251	1999	2021	2204	2185	1929	1938
14_g^+	2842	2891	2702	2736	2832	2830	2568	2585	2727	2749	2470	2478
16_g^+	3505	3552	3369	3392	3461	3442	3195	3205	3282	3344	3066	3073
18_g^+	4253	4253	4099	4108	4094	4083	3882	3881	3869	3967	3716	3721
20_g^+	4985	4989	4892	4882	4729	4749	4627	4613	4493	4611	4420	4422
22_g^+	5729	5757	5748	5715	5403	5437	5430	5400	5167	5276	5178	5176
24_g^+	6551	6555	6663	6605	6127	6143	6290	6241	5897	5957	5988	5983
26_g^+	7434	7379	7641	7552	6905	6867	7208	7136	6686	6652	6852	6841
28_g^+									7535	7360	7767	7751
0_β^+	478	590	649	753	500	537	647	712	492	581	665	682
2_β^+	861	809	863	993	856	797	860	939	844	822	878	900
4_β^+	1248	1173	1258	1425	1240	1185	1246	1347	1234	1198	1263	1291
6_β^+	1650	1632	1760	1967	1650	1652	1734	1859	1800	1655	1747	1782
8_β^+		2164	2348	2593	2118	2180	2303	2450		2173	2307	2348
10_β^+		2755	3013	3292		2755	2943	3111		2738	2934	2982
2_γ^+	677	840	858	856	668	805	849	847	649	817	859	860
3_γ^+	963	954	969	971	943	924	955	956	940	932	962	965
4_γ^+	1049	1101	1105	1110	1034	1079	1084	1087	1028	1080	1087	1090
5_γ^+	1315	1258	1263	1269	1306	1236	1234	1237	1307	1234	1230	1235
6_γ^+		1464	1440	1447	1438	1446	1402	1405	1463	1438	1391	1396
7_γ^+	1727	1653	1637	1642	1731	1630	1587	1589	1731	1617	1567	1572
8_γ^+		1909	1853	1854		1886	1789	1790		1866	1759	1764
9_γ^+	2198	2122	2087	2082		2088	2008	2005		2064	1965	1971
10_γ^+		2421	2338	2326		2382	2243	2236		2351	2186	2192
r.m.s. [keV]		58	108	128		47	156	164		83	155	151

TABLE IX: Excitation energies of the ground, β and γ band states J_i^+ with $i = g, \beta, \gamma$, for ^{186,188}Pt and ^{190}Pt yielded SSA, ISWSA, X(5), and SMA, ISWMA, Z(5), respectively, are compared with the corresponding experimental data taken from Refs. [34–36].

E [keV]	^{186}Pt			^{188}Pt			^{190}Pt			
J_i^+	Exp.	SSA	ISWSA	Exp.	SSA	ISWSA	Exp.	SMA	ISWMA	Z(5)
2_g^+	192	146	123	266	232	183	296	225	282	284
4_g^+	490	426	362	671	645	545	737	645	721	667
6_g^+	878	801	685	1185	1170	1045	1288	1206	1259	1130
8_g^+	1343	1250	1080	1783	1772	1667	1915	1872	1885	1668
10_g^+	1858	1757	1543	2438	2429	2405	2535	2620	2591	2276
12_g^+	2336	2315	2073	3105	3127	3256				
14_g^+	2825	2916	2667							
16_g^+	3395	3556	3325							
18_g^+	4051	4229	4045							
20_g^+	4788	4933	4827							
22_g^+	5597	5666	5671							
24_g^+	6464	6424	6575							
26_g^+	7408	7205	7540							
0_β^+	472	472	642	799	719	849	921	832	661	1110
2_β^+	798	743	856	1115	1193	1153	1203	1260	1173	1617
4_β^+	1223	1134	1247		1802	1716		1875	1931	2259
6_β^+	1600	1604	1744		2493	2446		2607	2815	2999
8_β^+		2135	2325		3240	3314		3426	3803	3822
10_β^+		2718	2982		4028	4308			4885	4724
2_γ^+	607	849	917	606	681	723	598	648	581	521
3_γ^+	957	970	1027	936	860	887	917	848	812	737
4_γ^+	992	1130	1161	1085	1098	1089	1128	1159	1183	1254
5_γ^+	1363	1290	1317		1316	1325	1450	1369	1391	1315
6_γ^+	1470	1505	1492	1636	1630	1594	1733	1808	1882	2004
7_γ^+	1801	1693	1687		1868	1893		2009	2062	1949
8_γ^+	2004	1954	1899	2247	2241	2223		2559	2665	2799
9_γ^+	2280	2163	2129		2489	2583		2742	2816	2644
10_γ^+	2545	2462	2377		2911	2971		3391	3222	3647
r.m.s. [keV]		107	155		45	89		71	98	206

TABLE X: Excitation energies, given in units of keV, of the ground, β and γ band states J_i^+ with $i = g, \beta, \gamma$, for ^{192,194,196}Pt yielded by SSM, ISWMA and Z(5) are compared with the corresponding experimental data taken from Refs. [37–39].

E [keV]	^{192}Pt				^{194}Pt				^{196}Pt			
J_i^+	Exp.	SSA	ISWSA	Z(5)	Exp.	SSA	ISWSA	Z(5)	Exp.	SMA	ISWMA	Z(5)
2_g^+	317	214	303	297	328	252	334	329	356	255	314	318
4_g^+	785	647	772	698	811	723	835	774	877	748	824	747
6_g^+	1365	1247	1346	1184	1412	1347	1435	1313	1526	1414	1466	1266
8_g^+	2018	1979	2010	1747	2100	2081	2120	1936	2253	2215	2227	1868
10_g^+	2729	2820	2759	2383	2848	2899	2883	2642	3044	3125	3101	2548
0_β^+	1195	1108	705	1163	1267	1150	785	1289	1135	948	722	1244
2_β^+	1439	1489	1254	1693	1512	1623	1392	1877	1362	1428	1288	1810
4_β^+		2117	2062	2366		2328	2272	2623		2138	2145	2530
6_β^+		2903	3005	3140		3165	3283	3482		2996	3165	3358
8_β^+		3807	4055	4003		4094	4398	4438		3969	4322	4280
2_γ^+	612	668	552	546	622	627	638	605	689	724	660	584
3_γ^+	921	877	798	772	923	868	909	856	1015	951	915	825
4_γ^+	1201	1184	1201	1313	1229	1284	1378	1456	1293	1280	1290	1405
5_γ^+	1482	1418	1418	1377	1499	1492	1590	1527	1610	1543	1560	1473
6_γ^+	1869	1865	1953	2099		2090	2214	2327	2007	2008	2051	2245
7_γ^+	2113	2106	2134	2041		2246	2360	2263		2286	2328	2183
8_γ^+	2591	2678	2792	2931		3004	3130	3250	2750	2870	2928	3134
9_γ^+		2914	2938	2769		3095	3211	3070		3151	3211	2961
10_γ^+		3597	3371	3819		3995	3665	4234		3841	3694	4084
r.m.s. [keV]		76	158	193		69	160	157		92	135	274

TABLE XI: The reduced E2 transition probabilities determined with the SSA, ISWSA and X(5) models for ^{180,182,184}Pt, are compared with the corresponding experimental data taken from Refs. [21, 31, 33].

B(E2) [W.u.]	^{180}Pt				^{182}Pt				^{184}Pt			
$J_i^+ \rightarrow J_f^{'+}$	Exp.	SSA	ISWSA	X(5)	Exp.	SSA	ISWSA	X(5)	Exp.	SSA	ISWSA	X(5)
$2_g^+ \rightarrow 0_g^+$	153^{+15}_{-15}	110	106	106	108^{+7}_{-7}	167	166	86	127^{+5}_{-5}	176	179	75
$4_g^+ \rightarrow 2_g^+$	140^{+30}_{-30}	168	169	169	188^{+11}_{-11}	226	222	138	210^{+8}_{-8}	238	236	119
$6_g^+ \rightarrow 4_g^+$	≥ 50	202	210	210	284^{+18}_{-18}	232	224	171	226^{+12}_{-12}	243	235	148
$8_g^+ \rightarrow 6_g^+$		230	241	241	253^{+20}_{-20}	221	215	196	271^{+18}_{-18}	232	222	170
$10_g^+ \rightarrow 8_g^+$		255	265	266	266^{+21}_{-21}	204	202	216	310^{+10}_{-10}	214	205	187
$12_g^+ \rightarrow 10_g^+$		278	285	286	158^{+18}_{-18}	185	189	232	183^{+17}_{-17}	193	188	201
$14_g^+ \rightarrow 12_g^+$		300	301	302	113^{+11}_{-11}	164	178	246	165^{+17}_{-17}	171	173	213
$16_g^+ \rightarrow 14_g^+$									143^{+17}_{-17}	150	159	223
$18_g^+ \rightarrow 16_g^+$									80^{+5}_{-5}	129	147	231
r.m.s. [W.u.]		36	39	39		47	52	80		43	49	86

TABLE XII: The reduced E2 transition probabilities of ^{186,188}Pt and ^{190}Pt, determined with SSA, ISWSA, and SMA, ISWMA, Z(5) respectively, are compared with the corresponding experimental data taken from Refs. [21, 35, 36].

B(E2) [W.u.]	^{186}Pt			^{188}Pt			^{190}Pt			
$J_i^+ \rightarrow J_f^{'+}$	Exp.	SSA	ISWSA	Exp.	SSA	ISWSA	Exp.	SMA	ISWMA	Z(5)
$2_g^+ \rightarrow 0_g^+$	113^{+8}_{-8}	162	162	82^{+15}_{-15}	82	82	56^{+3}_{-3}	56	56	56
$4_g^+ \rightarrow 2_g^+$	188^{+13}_{-13}	232	228		136	131		86	95	89
$6_g^+ \rightarrow 4_g^+$	289^{+23}_{-23}	254	248		171	162		119	138	123
$8_g^+ \rightarrow 6_g^+$	294^{+29}_{-29}	260	253		200	186		144	169	148
$10_g^+ \rightarrow 8_g^+$	304^{+26}_{-26}	259	254		226	205		166	191	166
$12_g^+ \rightarrow 10_g^+$	255^{+26}_{-26}	252	252		249	220				
$14_g^+ \rightarrow 12_g^+$	225^{+21}_{-21}	243	249							
$16_g^+ \rightarrow 14_g^+$	201^{+36}_{-36}	232	246							
r.m.s. [W.u.]		36	40							

TABLE XIII: The reduced E2 transition probabilities of ^{192,194,196}Pt determined with SMA, ISWMA and Z(5) respectively, are compared with the corresponding experimental data taken from Refs. [37–39].

B(E2) [W.u.]	^{192}Pt				^{194}Pt				^{196}Pt			
$J_i^+ \to J_f^{'+}$	Exp.	SMA	ISWMA	Z(5)	Exp.	SMA	ISWMA	Z(5)	Exp.	SMA	ISWMA	Z(5)
$2_g^+ \to 0_g^+$	$57.2^{+1.2}_{-1.2}$	49	41	42	$49.2^{+0.8}_{-0.8}$	25	20	26	$40.6^{+0.2}_{-0.2}$	34	28	32
$4_g^+ \to 2_g^+$	89^{+5}_{-5}	73	71	68	85^{+5}_{-5}	37	34	41	$60^{+0.9}_{-0.9}$	52	48	51
$6_g^+ \to 4_g^+$	70^{+30}_{-30}	98	103	94	67^{+21}_{-21}	51	49	57	73^{+4}_{-73}	72	70	70
$8_g^+ \to 6_g^+$					50^{+14}_{-14}	61	60	69	78^{+10}_{-78}	87	85	84
$10_g^+ \to 8_g^+$					34^{+9}_{-9}	70	68	77				
$2_\beta^+ \to 0_\beta^+$									5^{+5}_{-5}	23	20	25
$3_\gamma^+ \to 2_\gamma^+$	102^{+10}_{-10}	89	85	92								
$4_\gamma^+ \to 2_\gamma^+$					21^{+4}_{-4}	15	14	19	29^{+6}_{-29}	22	19	24
$6_\gamma^+ \to 4_\gamma^+$									49^{+13}_{-13}	29	28	33
$0_\beta^+ \to 2_g^+$					$0.63^{+0.14}_{-0.14}$	9.13	21.43	19.55	$2.8^{+1.5}_{-1.5}$	15.5	30.8	24
$2_\beta^+ \to 0_g^+$									$0.0025^{+0.0024}_{-0.0024}$	0.18	0.0033	0.34
$2_\beta^+ \to 4_g^+$									$0.13^{+0.12}_{-0.12}$	9.8	13.6	10.5
$0_\beta^+ \to 2_\gamma^+$					$8.4^{+1.9}_{-1.9}$	39.9	1.9	0	18^{+10}_{-10}	21	1	0
$2_\beta^+ \to 2_\gamma^+$									$0.26^{+0.23}_{-0.23}$	0.02	8	4.6
$2_\gamma^+ \to 0_g^+$	$0.55^{+0.04}_{-0.04}$	0.93	3.42	0	$0.29^{+0.04}_{-0.04}$	1.29	1.75	0				
$2_\gamma^+ \to 2_g^+$					89^{+11}_{-11}	71	87	42				
$3_\gamma^+ \to 2_g^+$	$0.68^{+0.07}_{-0.07}$	1.74	7.13	0								
$3_\gamma^+ \to 4_g^+$	38^{+10}_{-10}	38	38	53								
$4_\gamma^+ \to 2_g^+$					$0.36^{+0.07}_{-0.07}$	0.79	1.21	0	$0.56^{+0.12}_{-0.17}$	0.32	0.69	0
$4_\gamma^+ \to 4_g^+$					14	16	21	9				
$6_\gamma^+ \to 4_g^+$									$0.48^{+0.14}_{-0.14}$	0.19	0.41	0
$6_\gamma^+ \to 6_g^+$									16^{+5}_{-5}	5	9	6
r.m.s. [W.u.]		14	17	15		22	22	25		9	13	11

TABLE XIV: The branching ratios for some states of the ^{188}Pt and ^{190,192,194}Pt isotopes determined with SSA, ISWSA and SMA, ISWMA, Z(5), respectively, are compared with the corresponding experimental data taken from Ref. [40].

$\frac{B(E2;J^+\to J'^+)}{B(E2;I^+\to I'^+)}$	^{188}Pt			^{190}Pt				^{192}Pt				^{194}Pt			
$\times 10^2$	Exp.	SSA	ISWSA	Exp.	SMA	ISWMA	Z(5)	Exp.	SMA	ISWMA	Z(5)	Exp.	SMA	ISWMA	Z(5)
$\frac{2^+_\gamma\to 0^+_g}{2^+_\gamma\to 2^+_g}$	3.44	63	66	1.24	1.95	4.90	0	0.51	1.96	7.55	0	0.38	1.81	2.01	0
$\frac{3^+_\gamma\to 2^+_g}{3^+_\gamma\to 2^+_\gamma}$	4.5	23	17	1.8	2.2	6.0	0	0.76	1.95	8.42	0	0.5	5.37	9.04	0
$\frac{3^+_\gamma\to 4^+_g}{3^+_\gamma\to 2^+_\gamma}$		9.9	7.3	49	49	49	57	26	43	45	57		128	182	57
$\frac{0^+_\beta\to 2^+_g}{0^+_\beta\to 2^+_\beta}$	$\geq$11	23.2	17	11	14	31	19	3.8	8.1	31	19	7.9	10.5	31	19
$\frac{2^+_\beta\to 0^+_g}{2^+_\beta\to 0^+_\beta}$	0.83	0.37	3.17	0.02	0.82	0.02	1.39	0.022	1.16	0.017	1.39		1.04	0.02	1.39
$\frac{2^+_\beta\to 4^+_g}{2^+_\beta\to 0^+_\beta}$	19	66	49	4.2	44	68	42	$\leq$2.8	28	68	42		35	68	42
r.m.s.		35	32		16	27	16		13	30	22		3	14	7
t_2 [W.u.]$^{\frac{1}{2}}$		-316.8	-184.9		2931	145.2									

In Table XIV we list the results for branching ratios of few states from the γ and β bands obtained by SSA, ISWSA, SMA and ISWMA approaches, respectively. They are compared with the experimental data of Ref.[40]. For ^{190,192,194}Pt we list also the results yielded by the Z(5) formalism. The prameters detemining the transition operator were fixed as follows. For ^{188}Pt and ^{190}Pt we kept t_1 as given in Table IV and VI respectively, while t_2 was fixed by a least square procedure. The results for t_2 are also listed in Table XIV. As for the rest of isotopes from above mentioned Table, the parameters t_1 and t_2 are as listed in Table VI.

Another objective of the present work is to determine the shape of each considered isotope in ground and excited states, within both the SSA and the SMA. Indeed, it is interesting to see how the shape changes when one passes from one isotope to another and moreover whether this picture is state dependent.We expect to visualize the shape phase transition and also possible shape coexistence. The static shape is defined by the values of the intrinsic variables β and γ for which the probability density (the probability in the volume unit of $d\beta d\gamma$),

$$P(\beta,\gamma)=|f(\beta)\phi(\gamma)|^2\beta^4|\sin 3\gamma|, \tag{3.3}$$

reaches a maximum value. In Figs. 1-3, the contour plots are represented in the coordinates $(\beta\cos\gamma,\beta\sin\gamma)$. In order to save the space we chose two representatives for SSA, ^{180}Pt and

^{188}Pt, and one for SMA, ^{190}Pt. Indeed, the graphs corresponding to $^{182-186}$Pt are similar to that of ^{180}Pt and those of $^{192-196}$Pt resemble that of ^{190}Pt. We may ask ourself why to make such plots once we know that the power expansion in γ was performed around $\gamma = 0^0$ and $\gamma = 30^0$. We notice that the density maxima are met not in the same point where the potential is minimum. The reason is that the density accounts also for the kinetic energy and moreover includes a factor defining the measure of the integration in the β and γ coordinates. These figures reflect the structure of the wave functions. Indeed, since the γ dependent function depends on $\cos 3\gamma$ and the spheroidal functions are symmetric with respect to the space reflection transformation, the graphs exhibit the symmetry $\gamma \to \pi/3 - \gamma$. Concerning SMA the mentioned symmetry is caused by the fact the potential in γ is function of $cos^2 3\gamma$. Also, the node of the β function causes a doublet maxima with the same γ. For ^{188}Pt we notice equal density curves which surround two maxima of identical beta. This situation is specific to the phase coexistence. It is worth mentioning that such transition is showing up despite the fact the for all isotopes $^{180-188}$Pt we used a power expansion in γ around 0^0. That means that the transition is caused not only by the potential shape but also by the structure coefficients involved in the associated differential equations. Actually we calculated the spectroscopic properties of Pt isotopes with $A \geq 190$ also with a power expansion in γ around $\gamma = 0$. However, the results of SMA are characterized by a smaller r.m.s values for the deviations of the predictions from the experimental data. It is interesting to note that although we changed the description when we passed from ^{188}Pt to ^{190}Pt the probability density undergoes a smooth transition. The maxima surrounded by equidensity curves merge in one maximum at $\gamma = 30^0$ for ground and β band states while for γ band states the doublets are well separated. How this picture is modified when additional degrees of freedom like octupole [41, 42] or single particle [43, 44] will be analyzed elsewhere.

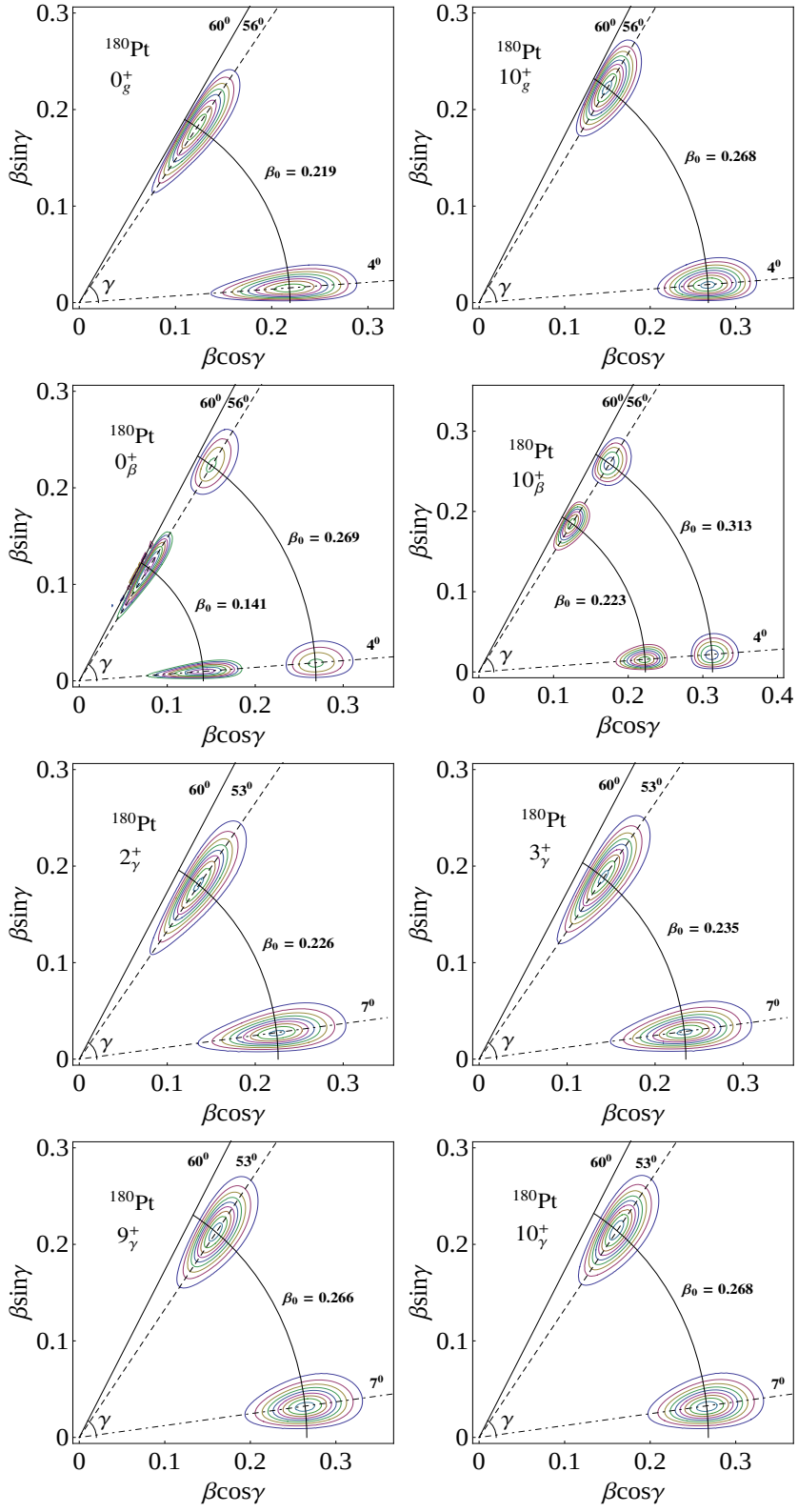

FIG. 1: (Color online) Probability densities for the states 0^+_g, 10^+_g, 0_β, 10_β, 2^+_γ, 3^+_γ, 9^+_γ and 10^+_γ of ^{180}Pt calculated with SSA.

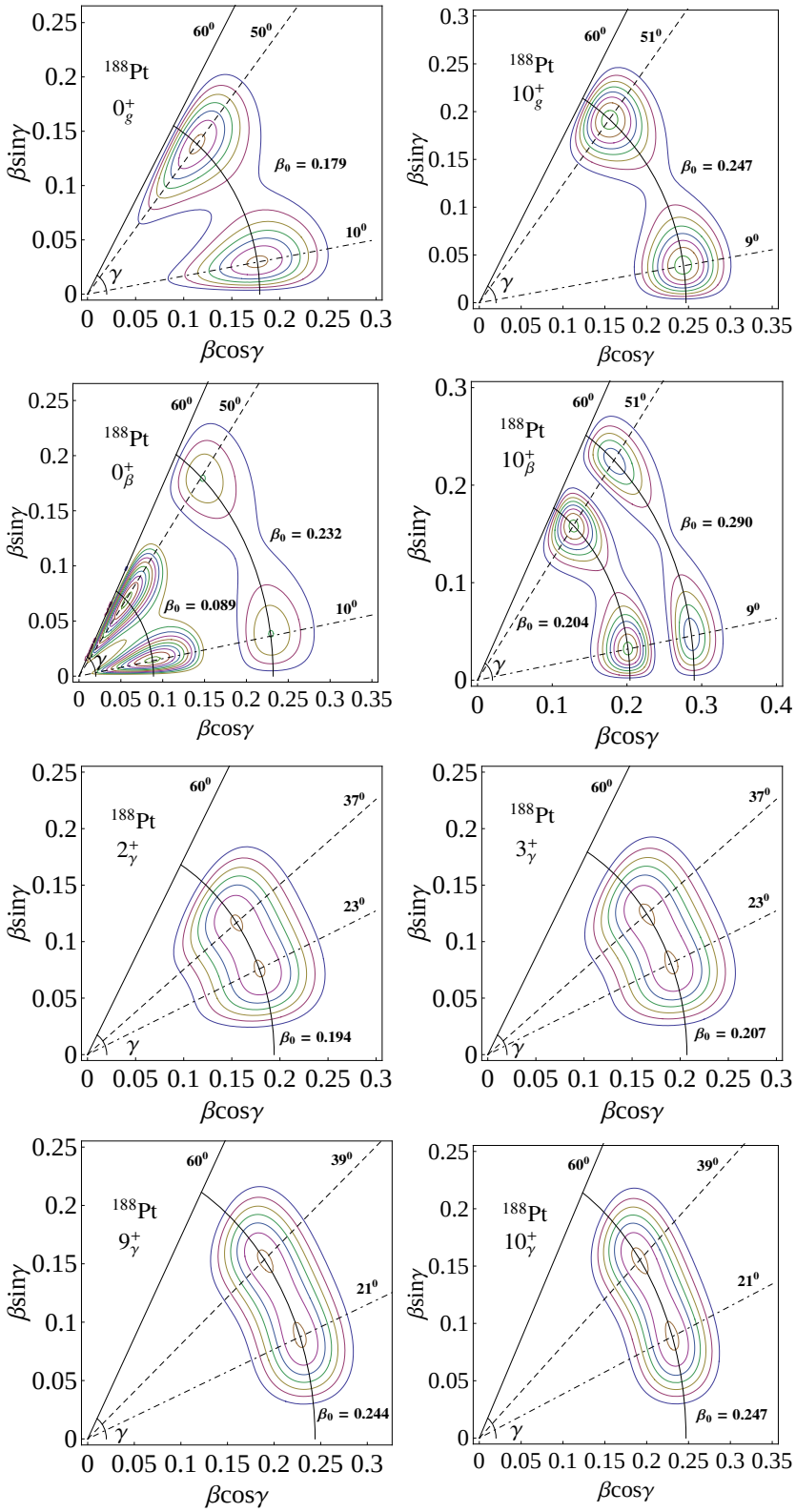

FIG. 2: (Color online)The same as in Fig. 1 but for ^{188}Pt.

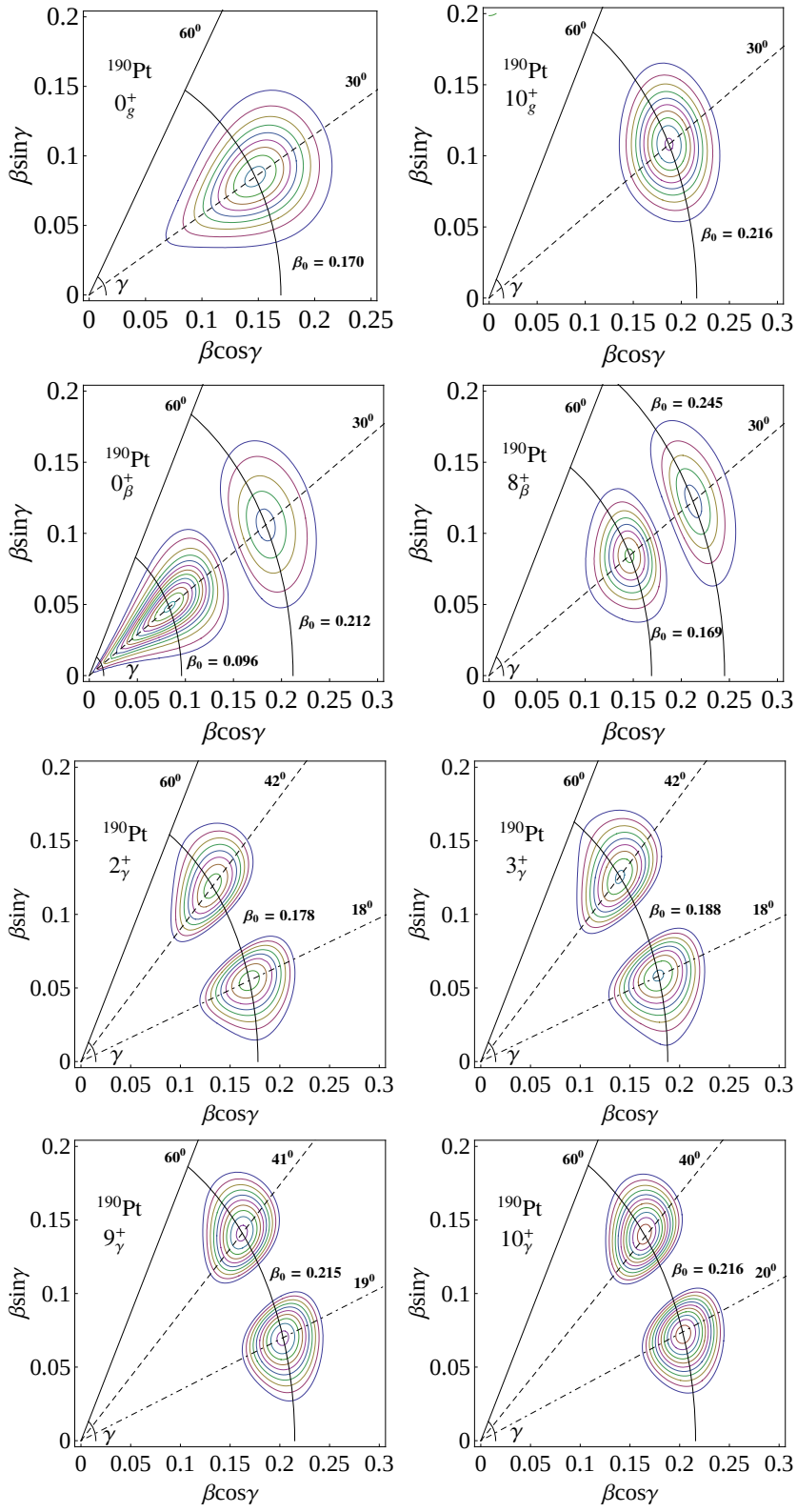

FIG. 3: (Color online) Probability densities for the states 0^+_g, 10^+_g, 0_β, 8_β, 2^+_γ, 3^+_γ, 9^+_γ and 10^+_γ of ^{190}Pt calculated with SMA.

IV. CONCLUSIONS

In the previous Section we described some even-even isotopes of Pt by four solvable models emerging from the generalized Bohr Mottelson Hamiltonian. Indeed for the isotopes with $180 \leq A \leq 188$ the approaches are those abbreviated by SSA and ISWSA, respectively, while for the rest of nuclei, $190 \leq A \leq 196$ the SMA and ISWMA are alternatively used. It is worth mentioning that the approach called ISWMA was used for the first time in the present paper. Since the first set exhibits some features of the $X(5)$ "symmetry" we compared the results of our calculations with those obtained with the X(5) formalism, if they are available. As for the other isotopes the results were compared with the $Z(5)$ results. One concludes that our results are slightly better than those obtained with X(5) and Z(5) methods regarding both the excitation energies and reduced transition E2 probabilities.

The wave function structure is nicely reflected in the contour plots for the probability density. It is suggested that due to the Hamiltonian symmetries the wave functions might be suitable for accounting for shape evolution as well as for possible shape coexistence.

Acknowledgment. This work was supported by the Romanian Ministry for Education Research Youth and Sport through the CNCSIS project ID-2/5.10.2011.

---

[1] A. Bohr, Mat. Fys. Medd. Dan. Vid. Selsk. **26** (1952) no.14; A.Bohr and B.Mottelson, Mat. Fys. Medd. Dan. Vid. Selsk. **27** (1953) no. 16.

[2] F. Iachello, Phys. Rev. Lett. **85** (2000) 3580.

[3] F. Iachello, Phys. Rev. Lett. **87** (2001) 052502.

[4] F. Iachello, Phys. Rev. Lett. **91** 132502 (2003).

[5] D. Bonatsos, D. Lenis, D. Petrellis, P.A. TerzievPhys. Lett. B **588**, 172 (2004).

[6] R. F. Casten and N. V. Zamfir, Phys. Rev. Lett. **87**, 052503 (2001).

[7] R. Krücken *et al.*, Phys. Rev. Lett. **88**, 232501 (2002).

[8] D. Tonev, A. Dewald, T. Klug, J. Jolie, O. Moller, S. Heinze, P. von Brentano, R. f. Casten, Phys. Rev C **69**, 034334 (2004).

[9] A. Dewald *et al.*, J. Phys. G: Nucl. Part. Phys. **31**, S1427 (2005).

[10] P. Petkov *et al.*, J. Phys.: Conf. Ser. **366**, 012036 (2012).

[11] A. A. Raduta and P. Buganu, J. Phys. G: Nucl. Part. Phys. **40**, 025108 (2013).

[12] A. A. Raduta, A. C. Gheorghe, P. Buganu and A. Faessler, Nucl. Phys. A **819**, 46-78 (2009).

[13] A. Gheorghe, A. A. Raduta and A. Faessler, Phys. Lett. B **648**, 171 (2007).

[14] A. A. Raduta, V. Ceausescu, A. Gheorghe and R. M. Dreizler, Nucl. Phys. A **381**, 253-276 (1982).

[15] A. A. Raduta and P. Buganu, Phys. Rev. C **83**, 034313 (2011).

[16] F. Iachello and A. Arima, *The Interacting boson model*, (Cambridge University Press, Cambridge, England) 1987.

[17] G. Gneuss and W. Greiner, Nucl. Phys. **171**, 449 (1971).

[18] G. Dracoulis *et al.*, J. Phys. G: Nucl. Phys. **12**, L97 (1986).

[19] G. D. Dracoulis, Phys. Rev. C **49**, 3324 (1994).

[20] U. Garg *et al.*, Phys. Lett. B **180**, 319-323 (1986).

[21] J. C. Walpe *et al.*, Phys. Rev. C **85** 057302 (2012).

[22] Liu Yuan *et al.*, Chinese Phys. Lett. **25**, 1633 (2008).

[23] K. Nomura, T. Otsuka, R. Rodrigues-Guzman, L. M. Robledo, P. Sarriguren, Phys. Rev. C **83**, 014309 (2011).

[24] L. M. Robledo, R. Rodriguez-Guzman and P. Sarriguren, J. Phys. G: Nucl. Part. Phys. **36**, 115104 (2009).

[25] L. Wilets and M. Jean, Phys. Rev.**102**, 788 (1956).

[26] L. Fortunato, Eur. J. Phys. A **26**, s01, 1-30 (2005).

[27] A. G. Ushveridze, *Quasi-exactly Solvable Models in Quantum Mechanics*, IOP, Bristol, 1994.

[28] M. E. Rose, Elementary Theory of Angular Momentum (Wiley, New York, 1957).

[29] A. A. Raduta, A. Gheorghe and Amand Faessler, Jour. Phys. G: Nucl. Part. Phys. **31** (2005) 337.

[30] A. S. Davydov and G. F. Filippov, Nucl. Phys. **8**, 237 (1958).

[31] S. -c. Wu and H. Niu, Nuclear Data Sheets **100**, 483 (2003).

[32] Balraj Singh and Joel C. Roedinger, Nuclear Data Sheets **111**, 2081 (2010).

[33] Coral M. Baglin, Nuclear Data Sheets **111**, 275 (2010).

[34] Coral M. Baglin, Nuclear Data Sheets **99**, 1 (2003).

[35] Balraj Singh, Nuclear Data Sheets **95** , 387 (2002).

[36] Balraj Singh, Nuclear Data Sheets **99**, 275 (2003).

[37] Coral M. Baglin, Nuclear Data Sheets **113**, 1871 (2012).

[38] Balraj Singh, Nuclear Data Sheets **107**, 1531 (2006).

[39] Huang Xiaolong, Nuclear Data Sheets **108**, 1093 (2007).

[40] M. Finger *et al.*, Nucl. Phys. A **188**, 369 (1972).

[41] V. Ceausescu and A. A. Raduta, Prog. Th. Phys. **52**, 903 (1974).

[42] A. A. Raduta *et al.*, Phys. Rev. **8**, 1525 (1973).

[43] A. A. Raduta, C. Lima and Amand Faessler, Phys. Lett. **121B**,1 (1983).

[44] A. A. Raduta, C. Lima and Amand Faessler, Z. Phys. A-Atoms and Nuclei **313**, 69 (1983).